14th Australasian Fluid Mechanics Conference
Adelaide University, Adelaide, Australia
10-14 December 2001

Parallel Simulation of Viscoelastic Flow Past an Array of Cylinders by a Unstructured FVM Algorithm

Hua-Shu Dou[1] and Nhan-Phan-Thien[2]

[1] School of Aeronautical, Mechanical and Mechatronic Engineering
The University of Sydney, NSW 2006, AUSTRALIA

[2]Department of Mechanical Engineering
The National University of Singapore, SINGAPORE 119260

Abstract

In this paper, the flow of an Oldroyd-B fluid past an array of circular cylinders in a channel is simulated by a parallelized pressure-based Finite Volume Method (FVM) using fine unstructured meshes. The numerical method is using the Discrete Elastic Viscous Split Stress vorticity (DEVSS-omega) formulation and the SIMPLER iteration algorithm. The spacing parameter between cylinders is selected L=6. The results show that the shear motion in the gap between the wall and the cylinder dominates the flow at high Deborah number. Closing of cylinders will alter the behaviour of wall shear layers and delay the occurrence of instability.

Introduction

Viscoelastic flows past an array of cylinders have been obtained much attention in the last decade due to its implicative applications in flows through porous media [3,8,10,11,14-16]. Experiments showed that this type of flows exhibits instability at high Deborah number [3,8,11]. Linear stability analysis also revealed the features of instability for various parameters [16,18]. Comparing to the flows past a single cylinder in a channel, it is well known that the extension in the wake of cylinders of array is reduced. How the shear behavior is changed is not clear. Experiments found that the critical Deborah number for instability increases with closing of the cylinders. Extension in the wake has been nominated as the mechanism for the instability initiation [2,11,12]. However, Dou and Phan-Thien [5] found that the mechanism for instability of viscoleastic flows past a single cylinder in a channel is generated by the strong shear on the cylinder rather than the elongation in the wake. The mechanism of instability in the case of array of cylinders needs to be carefully examined because of its importance in applications [6].

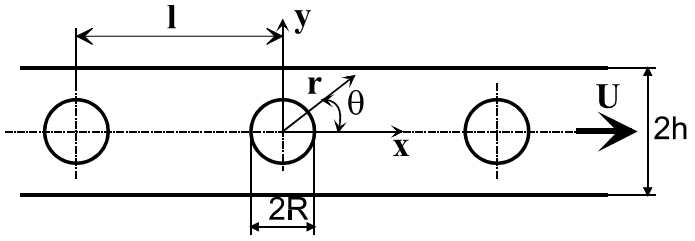

Fig.1 Sketch of the flow geometry

In this study, the flow of an Oldroyd-B fluid past an array of cylinders in a channel with geometry h/R=2 (Figure 1) is simulated using a parallelized unstructured FVM method, with fine meshes. The Discrete Elastic Viscous Split Stress (DEVSS) formulation is employed in the implementation of the SIMPLER pressure-velocity coupling method. The computing results are compared with those of single cylinder. The results show that the velocity inflection on the cylinder is delayed with the cylinder closing. This should contributes to the increasing of the critical Deborah number for instability occurrence. These results agrees qualitatively with the experimental behaviour reported in literature.

Governing Equations

The equations of mass and momentum conservation, and the constitutive equation for the Oldroyd-B model are [1,7]:

$$\nabla \bullet u = 0 \tag{1}$$

$$\rho\left(\frac{\partial u}{\partial t} + u \bullet \nabla u\right) = -\nabla p + \nabla \bullet \tau + \eta_N \nabla^2 u \tag{2}$$

$$\tau + \lambda\left(\frac{\partial \tau}{\partial t} - u \bullet \nabla \tau - \nabla u^T - \tau \bullet \nabla u\right) = 2\eta_{m0} D \tag{3}$$

where ρ is the fluid density, t the time, u the velocity vector, p the hydrodynamic pressure, η_N the solvent viscosity, $D=(\nabla u + \nabla u^T)/2$ the rate-of-strain tensor, η_{m0} a ``polymer-contributed" viscosity, $\lambda$ the (constant) relaxation time, and $\tau$ the ``extra" stress tensor, not necessarily traceless. By defining $\beta = \eta_{m0}/\eta_0$ as the retardation ratio, we have $\eta_N = \eta_0(1-\beta)$ For the UCM model, $\beta = 1$ and $\eta_0 = \eta_{m0}$. For the Newtonian fluid, $\beta = 0$ and $\eta_0 = \eta_N$. For the Oldroyd-B fluid $0 < \beta < 1$ and $\eta_0 = \eta_{m0}/\beta$. The rheological behaviours of these constitutive models have been discussed in (Bird et al [1], Huilgol and Phan-Thien [7]).

To stabilize the solution, the identity

$$\nabla^2 u = -\nabla \times \omega + \nabla(\nabla \bullet u) \tag{4}$$

is employed, where the vorticity $\omega = \nabla \times u$ With this, the momentum equations Eq.(2) are re-written as

$$\rho\left(\frac{\partial u}{\partial t} + u \bullet \nabla u\right) = -\nabla p + \nabla \bullet \tau + (\varepsilon + \eta_N)\nabla^2 u + \varepsilon \nabla \times \omega - \varepsilon \nabla(\nabla \bullet u) \tag{5}$$

where the value of ε can be adapted to the stress level. In this paper, we use a constant value of $\varepsilon, \varepsilon = \beta\eta_0$, and this formulation is named as DEVSS-ω scheme (Dou and Phan-Thien [4]).

All the dependent variables in the governing equations (3) and (5) can be written in the form of the general transport equations as

$$\frac{\partial(\Lambda\phi)}{\partial t} + \nabla \bullet (\Lambda u\phi - \Gamma \nabla\phi) = S_\phi = S_p\phi + S_c \tag{6}$$

where ϕ is one of the dependent variables, Γ denotes the diffusivity of ϕ, S_ϕ is the source term, and $(\Lambda u\phi - \Gamma\nabla\phi)$ is the ``flux'' of the variable ϕ. The source term is arbitrarily split in the manner shown on the right side of equation.

Numerical Method

Discretization of Equations

An unstructured FVM using pressure correction with triangular meshes (control volume-based finite-element method) is used to discretize the governing equations with a co-located mesh arrangement. The SIMPLER (Semi-Implicit Method for Pressure-Linked Equations Revised) algorithm is employed to couple the solution of these equations. Triangular meshes are generated in the computing domain (unstructured triangles of irregular size and shape). All the dependent variables such as velocities and pressure as well as stresses are stored at the vertices of the triangular elements. The velocities and stresses are interpolated over the elements using the same shape function, and the pressure and pressure correction are linearly interpolated over the elements. The formation of a typical control volume is shown in Fig.2, where the current node is denoted by P which is shared by six triangular elements ploted by the thick solid lines, and the surrounding nodes by A,B,C,D,E,F. The control volume for node P is constructed by connecting the centroids to the midpoints of the sides of the triangular elements sharing grid point P, forming a polygonal control volume(1-2-3-4-5-6-1).

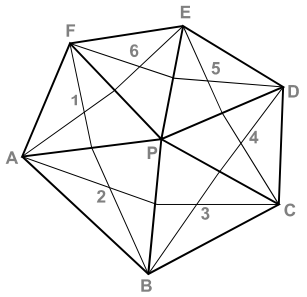

Fig.2 Control volume surrounding a computing node P.

Equation (6) (for velocities and stresses) is discretized by using the same interpolation function as in Prakash and Patankar [13]). A set of local coordinates (X,Y) is defined in the element, as shown in Fig. 3. The origin of this coordinate system (X,Y) is located at the centroid O, and the X axis is aligned with the element-average velocity vector U_{avg}, $U_{avg} = (U_1 + U_2 + U_3 / 3$. Here, ρ, Γ *and* S are assumed to be uniform over any triangular element, and the convection-diffusion flux is calculated by assuming that over any element ϕ varies exponentially in the direction of the average velocity vector and linearly in the normal direction. The shape function is

$$\phi = A\exp\left(\frac{\rho U_{avg} X}{\Gamma}\right) + BY + C \qquad (7)$$

where A,B and C are the coefficients in the interpolation formula.

The discretization of equation (6) is carried out using Eq.(7) in all the elements, then integration is performed over a control volume surrounding a node, the final discretization equation for the dependent variable ϕ can be expressed as

$$a_p\phi_p = \sum a_{nb}\phi_{nb} + b \qquad (8)$$

$$b = S_c\Delta V, \quad a_p = \sum a_{nb} - S_p\Delta V \qquad (9)$$

Here, the summation is to be taken over all the neighbouring nodes, aj are the combined convection-diffusion coefficients and b includes all the terms calculated explicitly, including the source terms, and nb denotes the neighbouring nodes. In addition, the source term is arbitrarily split into a combination of a constant term, and a linear term in ϕ, $S_c = S_p - S_c\Delta V$,

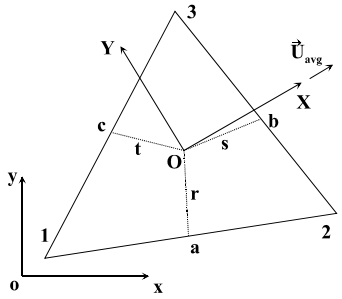

Fig.3 Local coordinates with a triangle element.

The discretization equations for pressure and pressure correction are obtained by applying the mass conversation principle over the surfaces of the control volume of a node and utilizing the momentum equations. The equal-order method proposed by Prakash and Patankar [13] is used in this study.

All of these algebraic equations are solved sequentially by using the SIMPLER iteration procedure with the Gauss-Seidel point solver. An under-relaxation technique is used to deal with the non-linearities of the equations. To improve the numerical stability of the constitutive equations, equal stress diffusion terms are introduced on both sides of equation, with a small dimensionless diffusivity of α (kept as a fraction of the De number, in this study α =0.02De was used); the terms on the left side are treated as the diffusion terms, and terms on the right side contribute toward the source terms.

Boundary Conditions

The computing domain is shown in Fig. 1, which is taken a unit cell around a cylinder. Periodic conditions for velocities, stresses and pressure are exerted on the inlet and outlet. No-slip conditions are imposed for u, v on solid surfaces. The boundary conditions on the solid surface for τ_{xx}, τ_{xy} *and* τ_{yy} are given by analytical solutions such as at the channel walls and the cylinder surface.

Parallel Algorithm

The parallel algorithm is detailed in (Dou and Phan-Thien [4]). The parallelization of the computations is implemented by means of a domain decomposition (DD) technique, using the master-slave communication model. In brief, the program was run on a distributed computing environment (called a workstation farm) consisting of 28 DEC Alpha 500/256. Communication is through a fast ethernet of 100 MBits per second. The message passing is supported by PVM software libraries version 3.4.1 from Oak Ridge National Laboratory.

Results and Discussion

The computation domain is shown in Fig.1; here, the dimensionless space parameter between the cylinders is L=l/R=6. The width of the passage is 2h=4R. An Oldroyd-B fluid with the viscosity ratio β =0.41 is used for the flow simulation. The Reynolds and the Deborah numbers are defined as: $\mathrm{Re} = \rho UR/\eta$ and $De = \lambda U/R$, where U is the average velocity

in the channel. The inertia terms are omitted in the present study (Re=0). Only steady flow is considered.

Mesh	Nnode	Nelem	$\Delta r / R$	$\Delta r / \Delta s$	DOF
M2	16546	32350	0.0048	0.30	115822
M3	17786	34760	0.0092	0.70	124502

Table 1. Meshes used for the computation.

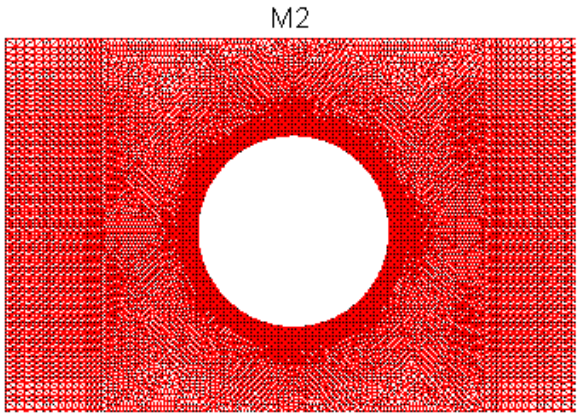

Fig.4 Mesh M2 used for this research.

Mixed meshes (structured and unstructured) are used for this study. Structured meshes are generated around the cylinder and at inlet and outlet, and unstructured meshes are generated elsewhere. Unstructured triangular meshes are adapted to the wake region and between the channel and the cylinder. Two meshes are presented in this paper. Fig. 4 shows the global view of the mesh M2 used in this study. Their key features are in Table 1, where Nnode and Nelem express the number of nodes and elements respectively, $\Delta r / R$ is the typical mesh size, defined as the ratio of the mesh size in radial direction on the cylinder surface to the cylinder radius, $\Delta R / \Delta s$ is the aspect ratio of meshes near the cylinder, and DOF stands for the degrees of freedom. High aspect ratio meshes are used near the cylinder for M2, while almost equal-lateral triangles are employed near the cylinder for M3. Mesh M2 is the same as the mesh M2 in [5] for -2<x<2 used for a single cylinder.

Mesh	M2			M3
De	Dec	De1	De2	Demax
single	0.6	1.10	1.60	0.6
Array	0.7	1.20	1.80	0.7

Table 2 Results for M2 and M3 and compared with [5].

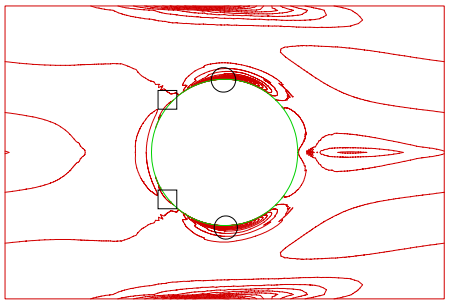

Fi.g.5 First normal stress difference at De=0.60 with M2.

Table 2 shows the computing results for M2 and M3. Dec denotes the velocity inflection appearance at the top of cylinder; De1 denotes that the computing is completely convergent; De2 denotes that the computation continues with oscillatory convergent history and finally breaking down. Demax is the maximum De number calculated with M3, just indicates a tendency of velocity inflection before divergence. This result suggests that Dec (Demax for M3) is the true margin of instability at which a steady solution is to be breakdown. M2 could pass through this margin is due to the more stability of the thin meshes for the numerical process. Any steady simulation results beyond Dec could not represent the physical flow of the fluid. Therefore, it is no sense to pursue a high De number solution for steady flow above Dec. In other hand, this suggests that numerical stability depends on the aspect ratio of meshes. Thin meshes introduce more approximation to the discretization, and generate more numerical diffusion. This numerical diffusion could increase numerical stability and delay the beakdown of solutions. This result about the effect of aspect ratio of meshes is consistent with the results of linear stability analysis [16].

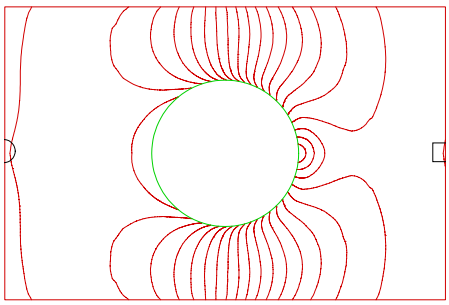

Fi.g 6 Pressure at De=0.60 with M2.

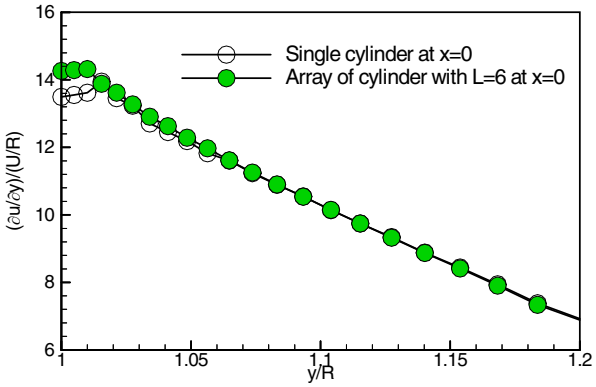

Fig.7 Velocity gradient near the cylinder at the plane x=0 in the gap at De=0.6 with Mesh M2.

The numerical results for the array of cylinders in Table 2 show that the maximum Deborah number can be extended to a higher range, comparing to the single cylinder case. This is agreement with the experiments that the critical Deborah number for instability increases with the closing of the cylinders [12]. Liu [11,12] think that the mechanism of instability is the extension in the wake, and cylinder approaching reduces the elongation in the wake. However, the numerical difficulty for De<1.0 is in the shear region on the top of cylinder, not in the wake for a single cylinder [5]. For De>1, the numerical difficulty is in the wake region. For reduced L, the numerical difficulty is more probably in the shear region for De<1. Therefore, the statement in the literature for the mechanism of instability is questionable.

Fig.5 and Fig.6 show the first normal stress difference and pressure respectively at De=0.60 with M2. Fig.7 shows the velocity gradient at the plane x=0 in the gap. A velocity inflection near the cylinder is clearly seen for both cases. Dou

and Phan-Thien [5] think that the velocity inflection in the shear layer is genereated by the cross-streamline pressure gradient resulted by normal stress. This will lead to the instability of shear flow and convected to the downsteam. The instability for this flow is caused by shear instability, not wake instability. Byars'[2] experiments showed that the instability exists in the shear region at shoulder of cylinder upstream the wake at high De. From Fig.7, it can seen that cylinder approaching delayed the velocity inflection. This should contributes to the stability extension to high De for reduces L.

Sureskumar [16] uses a linear stability analysis to explore the instability of Oldroyd-B fluid past a linear array of cylinders. They showed that the critical De number for instability increases with the increasing of the dimensionless parameter L of cylinder spacing. The results are: For L=2.5, Dec=0.64; For L=3, Dec=0.73; For L=3.5, Dec=0.86; For L=6, Dec=1.50 extrapolated; For L=30, Dec=7.70 extrapolated (This extrapolation is incorrect because there is no interaction between cylinders when L exceed a value). This is contradictive to the experiments [Liu, 12] which indicated that the critical De number for instability decreases with the increasing of the dimensionless parameter L. Therefore, the results of linear stability analysis is not reliable, although it can provide with some useful information sometimes. The authors think that the conflicting tendency is due to the Oldroyd-B is not suitable. Smith et al [14] improved the results in [16] using mesh refinement, but still lack of persuading.

Our simulation results show that with the reducing L (1) the stress shear layer on the cylinder becomes thinner; (2) the value of normal stress τ_{xx} within the layer becomes low; (3) the velocity inflection delays and is nearer the cylinder. These phenomena can be explained as follow. With the approaching of cylinders, the incoming flow to the cylinder is a no-recovered wake that is different from the full developed flow. The velocity gradient and normal stress on the cylinder depend on this incoming flow. In particular, the normal stress is history-dependent, not determined by the local velocity gradients only. On the other side, the shear layers on the channel walls opposite to the neighboring cylinders interact each other. This also has important influence on the stresses and pressure distribution on the walls. The low stress magnitude in the stress shear layer on the cylinder is the direct reason for delaying the velocity inflection and increases the Dec number. This will make the distortion of shear layer on the cylinder relaxed for closing space. Thus, this will delays the occurrence of velocity inflection on the cylinder and increases the Dec for instability. This simultaneously delays the disturbance of pressure in the shear layer and reduces the secondary flow near the cylinder surface. Therefore, the flow instability is dominated by the shear flow on the cylinder and the channel wall, not by wake elongation. This study supported the previous founding for single cylinder that the instability is due to an inflection velocity profile, near the cylinder, generated by normal stress on the cylinder surface at high De number, which can be captured with fine meshes only. Inflection velocity profile leads to flow instability according to Rayleigh theorem, and consequently allows to the convection of vortices within the shear layer downstream of the wake and results in the flow pulsation in the spanwise direction. Therefore, the origin of the instability is in the shear layer on the cylinder and not in the wake itself.

Conclusions

A detailed simulation is performed using mixed meshes for the flow of an Oldroyd-B fluid past an array of cylinder in a channel with h/R=2. The parallel computation was done in a distributed computing environment. This report focuses on the understanding of the physical problems at high De number. Numerical results obtained by the unstructured FVM algorithm and DEVSS-w formulation are compared qualitively with published results. The main conclusions of this study are as follows:

The numerical process stability is related to the mesh aspect ratio. This is consistent with the FEM linear instability analysis [14], in which it was shown that the rate of unstable perturbation increases with mesh aspect ratio.

The instability mechanism of viscoelastic flows past an array of cylinders is similar with a single cylinder, is dominated by shear flow, i.e., the inflection in the velocity at a critical De number (according to Rayleigh theorem). The pressure distortion near the cylinder due to the development of normal stress induces an inflection in the velocity and leads to the flow instability.

With the approaching of cylinders, the bahaviour of the shear layer on the cylinder changes. This change delays the occurrence of the velocity inflection on the cylinder and increases the Dec number for instability.

References

[1] R.B. Bird, R.C. Armstrong, and O. Hassager, Dynamics of Polymeric Liquids, Vol.1: Fluid Mechanics, 2nd ed.,Wiley, New York, 1987.

[2] J. A. Byars, Experimental Characterization of Viscoelastic Flow Instabilities, Ph.D thesis, MIT, Cambridge, MA 02139, USA, 1996.

[3] C. Chmielewski, and K. Jayaraman, Elastic instability in crossflow of polymer solutions through periodic array of cylinders, J. non-Newt. Fluid Mech., 48 (1993) 285-301.

[4] H.-S. Dou and N. Phan-Thien, The flow of an Oldroyd-B fluid past a cylinder in a channel: adaptive viscosity vorticity (DAVSS-omega) formulation, J. Non-Newt. Fluid Mech., 87 (1999) 47-73.

[5] H.-S. Dou and N. Phan-Thien, Viscoelastic flow past a confined cylinder: Instability and velocity inflection, J. non-Newt. Fluid Mech., 2000, submitted.

[6] Groisman and V. Steinberg, Elastic turbulence in a polymer solution flow, Nature, 405 (2000) 53-55.

[7] R.R. Huilgol and N. Phan-Thien, Fluid Mechanics of Viscoelasticity: General Principles, Constitutive Modelling and Numerical Techniques, Rheology Series Vol. 6, Elsevier, Amsterdam, 1997.

[8] Khomami, B, Moreno, LD., Stability of viscoelastic flow around periodic arrays of cylinders, Rheol. Acta, 36 (1997) 367-383.

[9] R.G. Larson, Instabilities in viscoelastic flows, Rheologica Acta, 31 (1992) 213-263.

[10] A.W. Liu, D.E. Bornside, R.C. Armstrong and R.A. Brown, Viscoelastic Flow of Polymer Solutions Around a Periodic, Linear Array of Cylinders: Comparisons of Predictions for Microstructure and Flow Fields. J. non-Newt. Fluid Mech., 77 (1998) 153-190.

[11] A.W. Liu, Viscoelastic Flow of Polymer Solutions Around Arrays of Cylinders: Comparisons of Experiments and theory, Ph.D thesis, MIT, Cambridge, USA, 1997.

[12] G.H. McKinley, P. Pakdel and A.Oztekin, Rheological and geometric scaling of purely elastic flow instabilities, J. non-Newt. Fluid Mech., 67 (1996) 19-47.

[13] C. Prakash and S.V. Patankar, A control volume-based finite-element method for solving the Navier-Stokes equations using equal-order velocity-pressure interpolation, Num. Heat Trans., 8 (1985) 259--280.

[14] M.D. Smith, R.C. Armstrong, R.A. Brown and R. Sureshkumar, Finite element analysis of stability of two-dimensional viscoelastic flows to three-dimensional perturbations, J. non-Newt. Fluid Mech., 93 (2000) 203-244.

[15] A. Souvaliotis, and A.N.Beris, Spectral collocation domain decomposition method for viscoelastic flow simulation in model porous geometry, Comp. Meth. App. Mech. Eng., 129 (1996) 9-28.

[16] Sureshkumar R, Smith MD, Armstrong RC, et al., Linear stability and dynamics of viscoelastic flows using time-dependent numerical simulations, J. non-Newt. Fluid Mech., 82 (1999) 57-104.